A low-carbon, funicular concrete floor system: design and engineering of the HiLo floors

Francesco Ranaudo, Tom Van Mele, Philippe Block

Block Research Group, ETH Zurich, CH

Contact: ranaudo@arch.ethz.ch

Abstract

This paper reports on the integrated computational design, engineering and construction of the concrete, rib-stiffened funicular floors of the HiLo research & innovation unit, built on the NEST platform in Dübendorf, Switzerland. These floors represent the first application of this innovative technology in a real project. The lightweight structural floors significantly reduce environmental impact and embodied carbon emissions, when compared to common reinforced concrete slabs, both by minimising material needs and by using a large percentage of recycled construction waste, thus additionally contributing to a circular economy in construction.

Keywords: concrete floors; slabs; rib-stiffened funicular floor; compression-only; embodied emissions; global warming potential; sustainable construction.

1 Introduction

Population growth combined with urbanisation will pose huge challenges to construction in the next decades. Most of this construction has historically happened in reinforced concrete, causing tremendous environmental issues, particularly towards global warming, due to the large greenhouse-gas emissions of cement and steel, but also accelerating the depletion of natural resources and virgin materials. Considering that for medium high-rises of ten to twenty floors, an average of 40% of the building mass is in the floors, this structural element is thus one of the most significant carbon emitters [1]. With billions of floors expected to be built by 2060 [2], this research developed an alternative, sustainable structural slab solution in concrete and implemented it for the first time in a real-scale office building.

This paper is structured as follows. In the first part of this section, a brief overview of the funicular floor system is provided, along with the main references for an in-depth review. Following, the HiLo unit and its two funicular floors are introduced. In Section 2, the design process is presented, from the form finding to the structural analyses. Section 3 shows the fabrication and construction of the floors. A comparison with more traditional structural floor systems is offered in Section 4. Finally, Section 5 presents a summary of the research and provides future outlooks.

1.1 Funicular floors background

Inspired by vaulted masonry structures, specifically those resulting from the tile-vaulting technique of Rafael Guastavino [3], the *funicular floor* is a structural slab system studied by the Block Research Group (BRG) since 2010. By using the principles of *strength through geometry* and *material effectiveness*, this system is able to reduce material and mass, promote the use of more sustainable materials, and improve longevity and circularity [4].

In a funicular floor the loads are transferred to the supports through arch action: a thin vault is designed to carry uniformly distributed loads in pure compression, while a set of ribs on the top of the vault accommodates concentrated loads and provides additional lateral stiffness against buckling. The horizontal thrust generated by the arch action is then resolved by tension ties connecting the support locations along the perimeter. These ties are usually post-tensioned to guarantee that they are already activated when the vaulted floor gets decentred and load is applied.

The BRG has investigated these concepts through a series of prototypes, briefly summarised in Table 1. Details about design and fabrication of these prototypes are given in [5–9].

However, the research and prototypes so far only studied small-scale elements, with simple support conditions and regular shapes. The HiLo floors are the first application of this disruptive technology at a meaningful scale in a real building project.

1.2 The HiLo unit

The opportunity to experiment at this scale was offered by the HiLo research & innovation unit built on the NEST platform in Dübendorf, Switzerland [10]. The NEST-HiLo (High performance, Low energy) unit aims to demonstrate innovations in the domains of lightweight construction as well as smart, integrated and adaptive building systems [11].

Two funicular floors have been designed and installed in the unit, shown in Figure 1 as Floor A, about 20 m^2, and Floor B, about 22,5 m^2, both with a maximum span of about 5,2 m.

While both floors are designed to integrate a Thermally Active Building System (TABS) embedding three loops of ⌀16 mm pipes within the section of their vaults, Floor B also features the integration of four air ducts for ventilation and a 3D-printed formwork. Details on the 3D-printed formwork and the building systems integration will be provided in separate publications, while here the focus will be on the structure.

Since the two floors share same design principles and similar dimensions, the remaining of this paper will refer to Floor A, if not specified otherwise.

Table 1. BRG funicular floor prototypes.

	SUDU	HiLo Prototype	3D-printed floor	WEF floor
	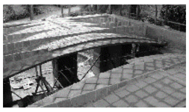		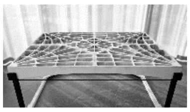	
Year	2010	2012 - 2016	2016-2018	2018 -2019
System	Rib-stiffened singly curved shell	Rib-stiffened doubly curved shell	Discretised rib-stiffened doubly curved shell	Double-layer rib-stiffened doubly curved shell
Supports	2, linear	4, corner	4, corner	4, linear
Material	Compressed stabilised earth block (CSEB) tiles	Self-compacting concrete (SCC) with 12mm steel fibres	3DP sand bonded by phenolic binder	Recycled SCC with 6mm steel fibres
f_{ck}	4 MPa	145 MPa	12 MPa	40 MPa
Installation	Built on site	Prefabricated	Prefabricated in modules	Cast in-situ
Formwork	No formwork	Double-side mould	Direct 3DP - No formwork	3D-printed and CNC cut moulds
Structural test	No	Yes	Yes	No
Building Systems	No integration	No integration	No integration	Hydronic coil
Reference	[5]	[6,7]	[8]	[9]

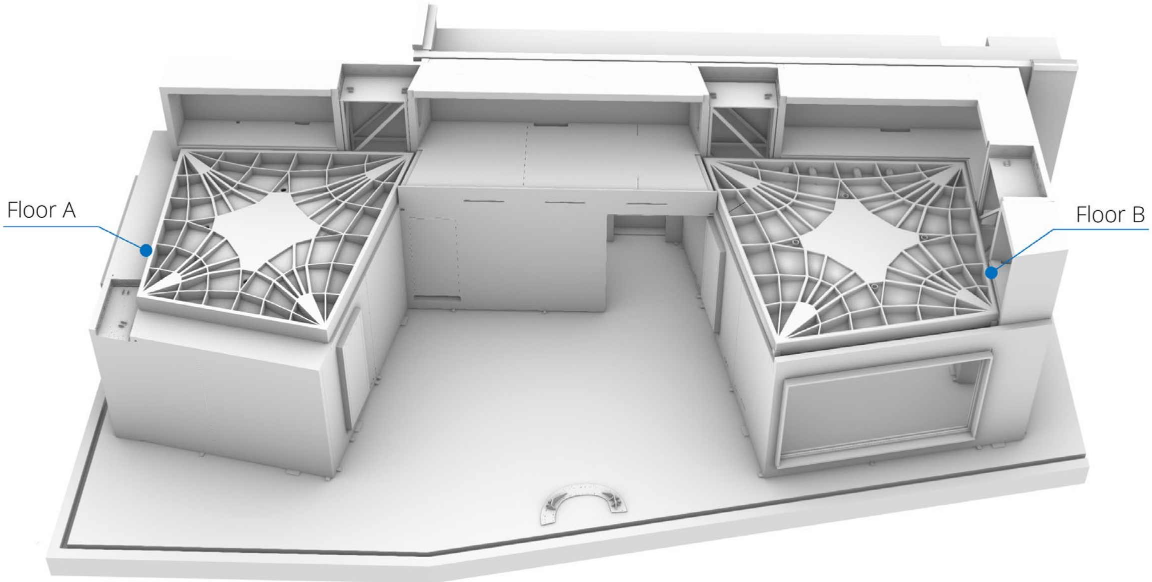

Figure 1. 3D view of the internal structure of the first floor of the HiLo unit, showing the structures of the two funicular floors designed and implemented in this research.

2 Design and engineering of the HiLo floors

This section describes the design and engineering of the funicular floors implemented in the HiLo unit: the form finding of the floors is presented in Section 2.1, and their final geometry is shown in Section 2.2; Section 2.3 offers an overview of the structural properties of the custom concrete mix used in this project; finally, Section 2.4 discusses the Finite Element Analysis (FEA) model and the results of the analyses.

2.1 Form finding

The geometry of the floors has been derived using a combination of Thrust Network Analysis (TNA) [12], topology optimisation [13] and FEA.

The form-finding procedure starts with the creation of a compression-only surface structure using TNA. This algorithm, made available through the *compas_tna* [14] package of COMPAS [15], requires the following inputs:

1. Target height of the structure;
2. Vertical loads on the structure;
3. Planar projection of the force network (form diagram).

The target height for the algorithm is the height of the vault's apex. Because of the architectural requirements on the inter-story height, the total height of the structural floors was constrained to 350 mm. The target height was then set to 275 mm, considering 50 mm for the thickness of the vault (see Section 3) and an additional 50 mm for fire protection and acoustics.

The loads on the structure are its self-weight and the additional uniformly distributed load in accordance with the structural codes.

The rib pattern, which corresponds to the form diagram in the TNA algorithm, can be any planar mesh with convex faces. In previous research on the funicular floors, this was inspired by historic ribbed masonry vaults [6,7] or programmatically generated through numerous iterations [8]. For the HiLo floors, similar strategies were used to generate the initial topology, but the pattern was then refined through a compliance-based topology optimisation algorithm. By evaluating the material distribution for several volume fractions (Figure 2), it was possible to identify the regions of the slabs where to increase (or decrease) the density of the ribs.

Finally, the ribs are generated as simple vertical extrusions along the network edges of the compression-only vault.

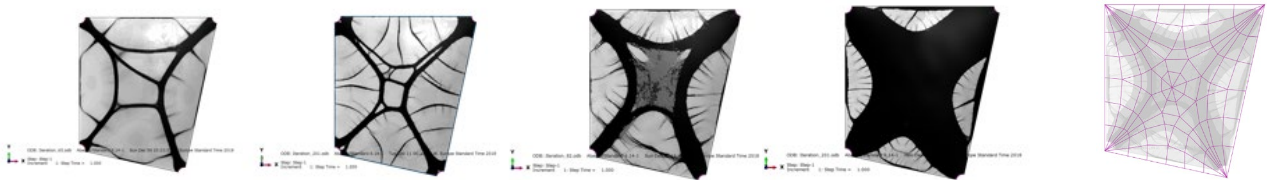

Figure 2. Topology optimisation studies for Floor A. The plots show the distribution of material that maximises stiffness for several volume fractions: 0,2 , 0,3 , 0,5 , and 0,7 (from left to right). On the right: overlay of the topology optimisation results and final pattern for TNA (in magenta).

2.2 Geometry

As noticed before, the elements' thicknesses were largely imposed by fabrication constraints:

- the minimum thickness of the ribs was set to 25 mm to allow a good flow of the concrete;
- since the vault had to include the ⌀16 mm pipes of the hydraulic system, its thickness was set to 50 mm to guarantee enough cover; and,
- the thickness of the primary and boundary ribs was derived from the FE analysis and set to 50 mm and 80mm, respectively.

The region in the centre of the floors was kept solid to both improve dynamic behaviour [16] and ease the fabrication process (see Section 3).

The final geometry is shown in Figure 3. The volume of concrete of the structural floors is 2,05 m^3 for Floor A and 2,30 m^3 for Floor B.

The post-tensioning was applied by means of four ⌀12 mm unbonded steel rods embedded in the boundary ribs, which transfer the force to the concrete structures through angular steel plates in the corners (Figure 4).

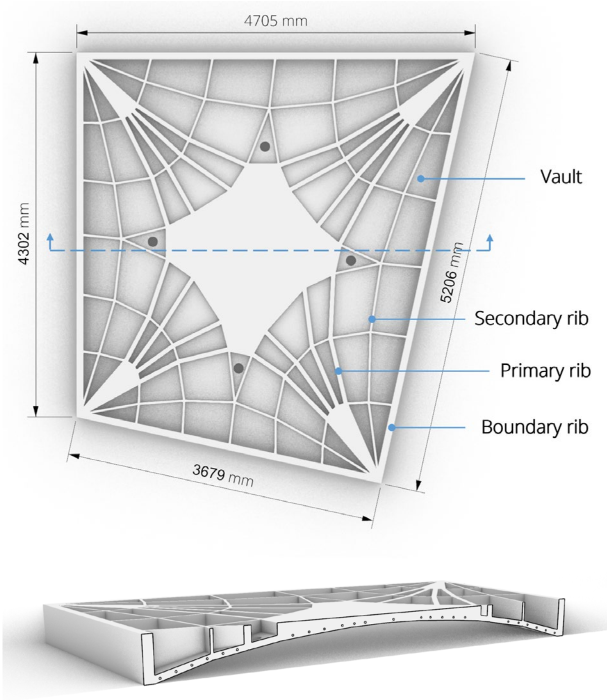

Figure 3. Final geometry of Floor A: top view (top), and perspective section (bottom).

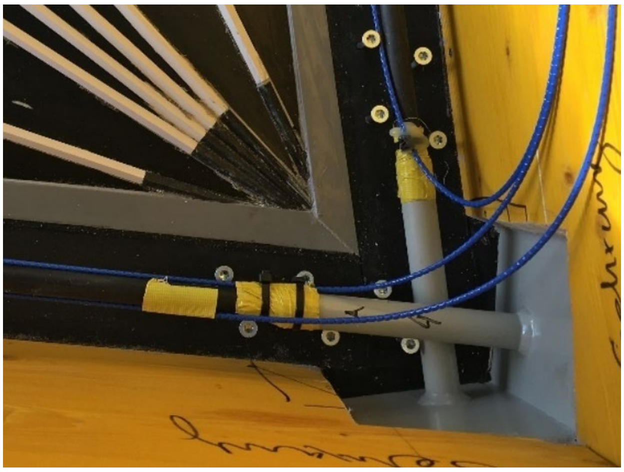

Figure 4. Detail of the ⌀12 mm post-tensioning rods and their anchoring system.

2.3 Concrete mix

A custom, self-compacting concrete mix was developed by Holcim (Schweiz) AG and BASF Schweiz AG specifically for this project, which used recycled concrete construction waste for more than half of its content, while still offering the extreme workability needed to fill the intricate mould geometry of the floor.

The structural properties for the concrete mix are summarised in Table 2.

Table 2 - Concrete material properties.

Cement	Susteno 3R
Cement Strength Class	32.5R
Fibers	SF OL 6/0.16
Density [kg/m³]	2334
Modulus of Elasticity [MPa]	32085
Characteristic Compressive Capacity, f_{ck} [MPa]	33.2
Characteristic Tensile Capacity, f_{ct} [MPa]	3.0
Poisson's ratio	0,17
90-day shrinkage [microstrain]	-565

2.4 Finite Element Analyses

The form-found geometry of the floors was then modelled in the finite element software Abaqus [17] to simulate the behaviour of the structure.

2.4.1 Model

The slabs were meshed using C3D10 solid elements with a max element size of 50 mm.

The boundary conditions were modelled to capture the unilateral (compression-only) supports along the edges.

The loads were applied and combined according to the Swiss standards for office buildings [18]: in addition to the structure self-weight (DL), a superimposed dead load (SDL) of 1 kPa and a uniformly distributed live load (LL) of 3 kPa were applied to the model.

2.4.2 Analysis results

The analysis model was firstly used to calibrate the level of post-tensioning.

The graph in Figure 5, obtained by simulating the deflection of the centre of the slab under dead load (1,0 DL + 1,0 SDL) for several levels of the post-tensioning force, shows that for a post-tensioning force of about 90 kN the deflection is completely restored. The final force was then set to 120 kN on each side to also account for tension losses. It is worth mentioning that the floor is already in a state of almost pure compression with about half of the final post-tensioning force.

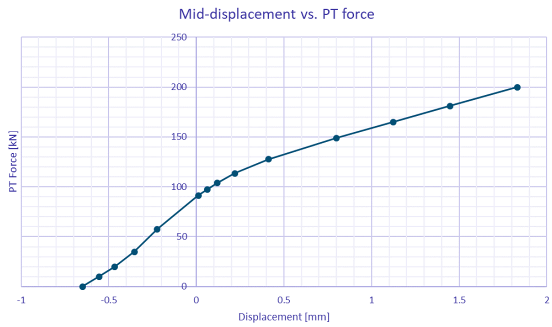

Figure 5. Deflection at the centre of the floor under dead loads (1,0 DL + 1,0 SDL) in service conditions for increasing levels of the post-tensioning force. The deflection is null for about 90 kN of post-tensioning force.

The stress state under ultimate conditions is shown Figure 6: the maximum compressive stresses were overall 10 MPa (about 1/3 of the material capacity), with some exceptions around the post-tensioning application points, suggesting that further material reductions or a concrete with an even lower cement content, and therefore less carbon intensive, would have been possible.

The deflections under service loads (Figure 6), were also extremely low and well below usual building limits: this is an inherent characteristic of an arching structure.

Since the characteristic compressive strength of the material was lower than 50 MPa, the floors were not required to be checked against concrete spalling according to the Swiss regulation: this is another advantage of using low-strength concrete materials.

3 Fabrication and Construction

This section describes the construction of the floors, from the fabrication and assembly of the formwork to casting on site.

For this first-time application the focus was on the structure and the optimisation of the formwork was not part of the scope of the project.

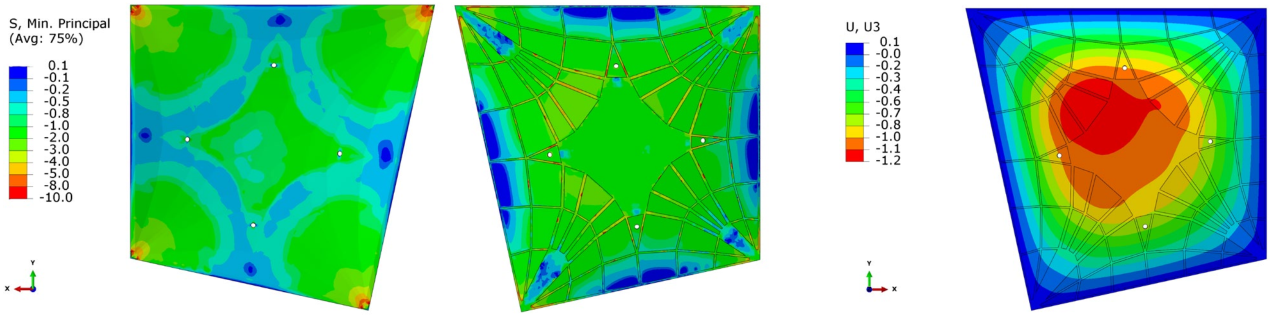

Figure 6. Stresses and deflections from the FEM model. From left to right: minimum principal stresses [MPa] under ultimate conditions in the bottom and top of the floor; vertical deflections [mm] under service conditions.

The formwork for each slab is comprised of two sides:

- a top formwork, similar in both floors, used to create the ribbed structure as well as to attach the TABS; and
- a bottom formwork, different between the two floors, needed to create the doubly curved vault shuttering surface.

The top formwork for both floors was designed and fabricated by the BRG. Because of on-site space constraints, it was divided into three parts: the discretisation was dictated by the loops of the pipes for the TABS, which could not be interrupted.

Each part of the top formwork consisted of a 16 mm layer of OSB laser-cut to guide the positioning of the CNC wire-cut polyurethane foam blocks, which were simply screwed to it. The blocks remained part of the final floors as insulating material, while the OSB was removed after casting. The foam blocks were cut with specific indents to precisely position the supporting plates for the pipes. The three parts of the top formwork were pre-assembled on site and then individually craned to their final positions (Figure 7).

The bottom formwork for Floor A was designed, fabricated and installed by the BRG. It consisted of 3mm Low Density Polyethylene (LDPE) panels, supported by CNC wire-cut polyurethane foam; the panels are seamed together by cut-to-size triangular PVC profiles connecting 3D-printed ABS joints placed at each node: the geometry of the seams and the nodes was chosen to recreate a visual reference of the force network, indented in the final geometry of the floor (Figure 9), but a simpler detail would have also been possible.

The complex design of this formwork aimed to create a better integration with the hydraulic system to enhance its heating and cooling performance; it also featured the direct inclusion of 3D-printed PLA air ducts for the ventilation system embedded within the structure itself.

Figure 7. Top formwork (part) during lifting. It is possible to notice the foam blocks creating the ribbed geometry and the ⌀16 mm pipes.

Figure 8. Positioning of the top formwork: one of the three parts of the pre-assembled formwork is craned in place. (photo by Juney Lee)

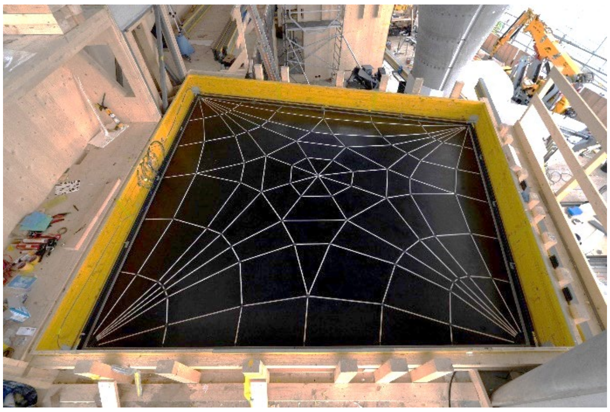

Figure 9. Floor A bottom formwork: the PE-LD panels in black and the triangular PVC profiles in white. (photo by Juney Lee).

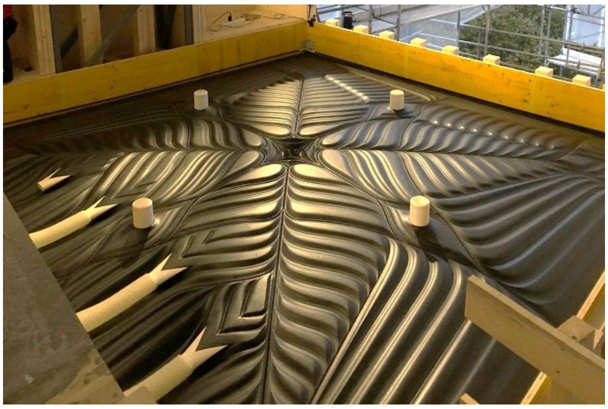

Figure 10. Bottom formwork of Floor B: the 3D sand-printed elements in black; the 3D-printed PLA air ducts and lights placeholders in white. (photo by Angela Yoo)

Figure 11. Floor A directly after demoulding.

Figure 12. Floor B directly after demoulding.

The ventilation system has been developed by the Architecture and Building Systems (A/S) chair at ETH Zurich.

The self-compacting concrete was poured from the middle of the slabs and smoothly flowed through the ribs, helped by the curved bottom geometry. The concrete did not need external vibration and only minor adjustments were made to control the top surface levelling.

The bottom vaulted surfaces of the floors, directly after demoulding, are shown in Figure 11 and Figure 12.

4 Impact

Here, we present a comparison of the HiLo floors against more traditional concrete floor systems designed for the same span and use. It is important to notice that some of these structural slabs would not be adequate to fit the nonstandard floor plan of the HiLo floors. Moreover, the HiLo floors have embedded Mechanical, Electrical and Plumbing (MEP) systems, which was not considered or even not possible for the other slabs analysed.

The calculations regarding GWP are based (for all the slabs) only on the structural materials and do not consider the contributions of the formwork, transportation and installation of the slabs: therefore, they are not supposed to be representative of the real environmental impact. The unit values for the GWP, which are taken from [19], are summarised in Table 3.

Even though the HiLo floors use 50% less concrete than a standard flat slab, this reduction is less than in previous prototypes and it can be mostly linked to the fabrication constraints, the integration of the building systems and the conservative assumptions for this first implementation.

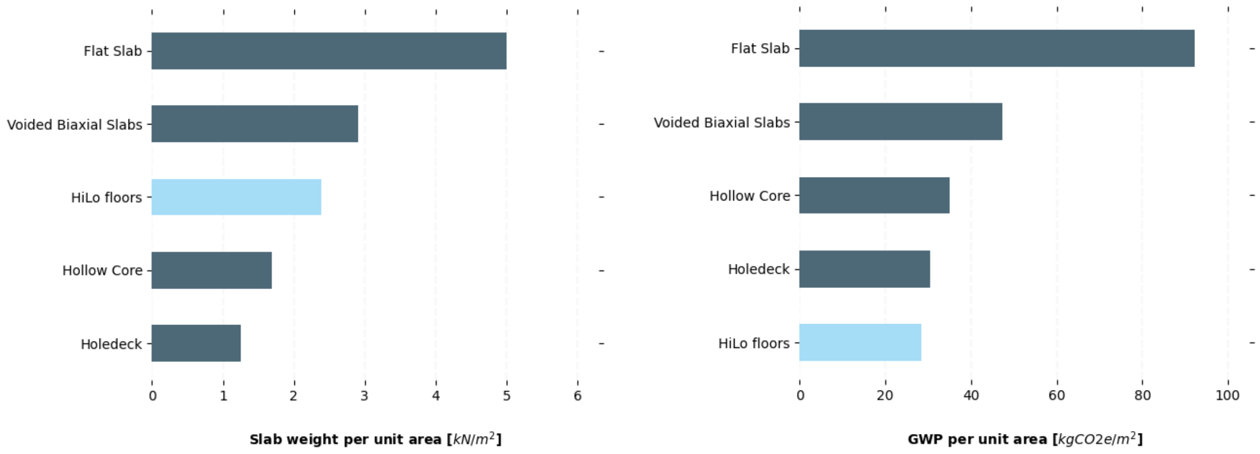

Figure 13. Comparison of the HiLo floors against more conventional structural concrete slabs in terms of weight (left) and GWP (right) per unit area

The HiLo floors performed better than all the other slabs in the comparison regarding GWP. The low GWP is explained by considering that, besides the limited amount of steel fibres in the concrete mix, the funicular floors are unreinforced; the post-tensioning rods and plates (Figure 4) correspond to only about 10% of the reinforcement that would be required in a conventional flat slab. This unique characteristic of the funicular floors also practically eliminates the risk of corrosion damage and fire, hence improving the longevity of the structure, while at the same time enabling a much more efficient recycling.

Table 3. Assumed Global Warming Potential (GWP) per unit mass of the structural materials.

Standard concrete [kgCO2e/kg]	High-strength concrete [kgCO2e/kg]	Reinforcement steel [kgCO2e/kg]
0.112	0.172	1.20

A more comprehensive comparison, also including the benefits of the reduced mass on the main structural elements, is currently under investigation by the authors and will be shared in future publications.

5 Conclusions

This paper presented the first application of the funicular floor system to a real-scale office building, from the conceptual design and engineering to their fabrication and installation on site.

The procedures for the form finding of the floors were explained and the structural simulations results discussed. It was shown that, even at a larger scale, the funicular floor system can safely comply with the structural building codes.

Details of formwork for such a complex geometry were also discussed, together with the main steps of the construction process. Even though outside the scope of the project, the complexity of the formwork remains a bottleneck of the system and requires further improvements. For this reason, prefabrication seems to be a more suitable option.

Finally, a comparison of the HiLo floors against other common structural concrete slabs showed the potential of the funicular floors to be a valid and sustainable alternative: low GWP, easily recyclable, and offering the introduction of low-pollution materials with high recycled content.

6 Acknowledgements

This project has been supported by Dr Max Rössler, Empa, NCCR DFAB and the ETH Zurich Foundation.

The authors would like to thank the project partners: DBT, A/S, ROK - Rippmann Oesterle Knauss GmbH, BEUP - Borgogno Eggenberger + Partner AG, Bürgin Creations, Holcim (Schweiz) AG and BASF Schweiz AG.

The authors are also grateful to Michael Lyrenmann, Dominik Werne, Minu Lee, Rafael Pastrana, Sandy Fenton, Aurèle Gheyselinck, Keerthana Udaykumar, and Chaoyu Du for their assistance during the prototyping and fabrication of the floors.

7 References

[1] Block P, Calvo Barentin C, Ranaudo F, Paulson N. Imposing Challenges, Disruptive Changes: Rethinking the Floor Slab. In: Ruby I, Ruby A, editors. *The Material Book*. Ruby Press; 2020.

[2] Dean B, Dulac J, Petrichenko K, Graham P. *Towards a zero-emission, efficient, and resilient buildings. Global Status Report*. 2016.

[3] Ochsendorf J. *Guastavino vaulting : the art of structural tile*. Princeton, NJ: Princeton Architectural Press; 2010.

[4] Block P, Van Mele T, Rippmann M, Ranaudo F, Calvo Barentin C, Paulson N. Redefining structural art: strategies, necessities and opportunities. *The Structural Engineer*. 2020 Jan;66–72.

[5] Block P, Davis L, DeJong M, Ochsendorf J. Tile vaulted systems for low-cost construction in Africa. *African Technology Development Forum*. 2010;**7**(1):4–13.

[6] López López D, Veenendaal D, Akbarzadeh M, Block P. Prototype of an ultra-thin, concrete vaulted floor system. In: *IASS-SLTE 2014 Symposium*. 2014.

[7] Liew A, López DL, Van Mele T, Block P. Design, fabrication and testing of a prototype, thin-vaulted, unreinforced concrete floor. *Engineering Structures*. 2017;137:323–35.

[8] Rippmann M, Liew A, Van Mele T, Block P. Design, fabrication and testing of discrete 3D sand-printed floor prototypes. *Materials Today Communications*. 2018; 15(June 2017):254–9.

[9] Jipa A, Calvo Barentin C, Lydon G, Rippmann M, Chousou G, Lomaglio M, et al. 3D-Printed Formwork for Integrated Funicular Concrete Slabs. *Proceedings of the IASS Annual Symposium 2019 – Structural Membranes*. 2019.

[10] Richner P, Heer P, Largo R, Marchesi E, Zimmermann M. NEST - A platform for the acceleration of innovation in buildings. *Informes de la Construccion*. 2017 Dec 30; **69**(548):1–8.

[11] Block P, Schlueter A, Veenendaal D, Bakker J, Begle M, Hischier I, et al. NEST HiLo: Investigating lightweight construction and adaptive energy systems. *Journal of Building Engineering*. 2017. 12:332–41.

[12] Block P, Ochsendorf J. Thrust network analysis: A new methodology for three-dimensional equilibrium. In: *Journal of the International Association for Shell and Spatial Structures*. 2007. p. 167–73.

[13] Sigmund O, Maute K. Topology optimization approaches A comparative review. *Struct Multidisc Optim.* 2013. 48:1031–55.

[14] Van Mele T. *COMPAS TNA: Implementation of Thrust Network Analysis based on COMPAS.* Available from: https://doi.org/10.5281/zenodo.3979410

[15] *COMPAS: A framework for computational research in architecture and structures*. Available from: http://compas.dev

[16] Wu H, Liew A, Van Mele T, Block P. Analysis and optimisation of a rib-stiffened vaulted floor for dynamic performance. *Engineering Structures.* 2020 Jun 15. 213.

[17] *Abaqus Unified FEA - SIMULIA™ by Dassault Systèmes®*. [cited 2021 Jan 27]. Available from: https://www.3ds.com/products-services/simulia/products/abaqus/

[18] *Swiss building codes SIA Zurich. SIA 261: actions on structures*. Schweizer Norm – Swiss Society of Engineers and Architects; 2003.

[19] *Embodied Carbon Footprint Database - Circular Ecology.* [cited 2021 Jan 21]. Available from: https://circularecology.com/embodied-carbon-footprint-database.html